# VISSR ATMOSPHERIC SOUNDER

Monthly Progress Report No. 3
For the period 1 Nov. 1973 to 30 Nov. 1973

Contract No. NAS5-21965

For National Aeronautics and Space Administration
Goddard Space Flight Center
Glen Dale Road
Greenbelt, Maryland 20771

by

V. E. Suomi, Principal Investigator
L. A. Sromovsky, Co-Investigator

The University of Wisconsin
Space Science and Engineering Center
1225 West Dayton Street
Madison, Wisconsin 53706

TABLE OF CONTENTS

## I. Introduction

With the general agreement to proceed with the "2 + 2 + 2" detector configuration described in last month's progress report on NAS5-21965 it became possible to concentrate on specific details of this configuration, in terms of radiometric performance, operation, data transmission, and data processing. Work in these areas is described in the following sections.

Additional work on data processing is underway in two areas: (1) use of visible and IR channels together to correct for clouds; and (2) application of McIDAS capabilities to sounder data processing. Both of these will be reported on later as meaningful results become available.

## II. Detector Configuration

The detector set consists of three pairs of detectors sampled two at a time: (1) two HgCdTe detectors each with square IGFOV's of 0.192mr x 0.192mr; (2) two HgCdTe detectors with IGFOV's of 0.384mr x 0.384mr; and (3) two InSb detectors with IGFOV's of 0.384mr x 0.384mr. The geometrical relationships between these sets is shown in Figure 1.

The two small detectors, used primarily for imaging in the 11.2μ window, are arranged to scan adjacent 0.192mr swaths which cover, without overlap, the 0.384mr swaths scanned by the large detectors. The large HgCdTe detectors are separated by .384mr edge to edge in the N-S direction (two 0.192mr swaths) and by the same spacing in the E-W direction as the small detectors (to simplify correction for sampling offsets). The InSb detectors have the same geometry as the large HgCdTe detectors except for an E-W translation which is a minimum consistent with required spacing for fabrication of the detector array and cold filter. In order that all scan lines can be E-W aligned by shifting an integral number of samples the center to center spacing of detectors in the E-W direction was chosen

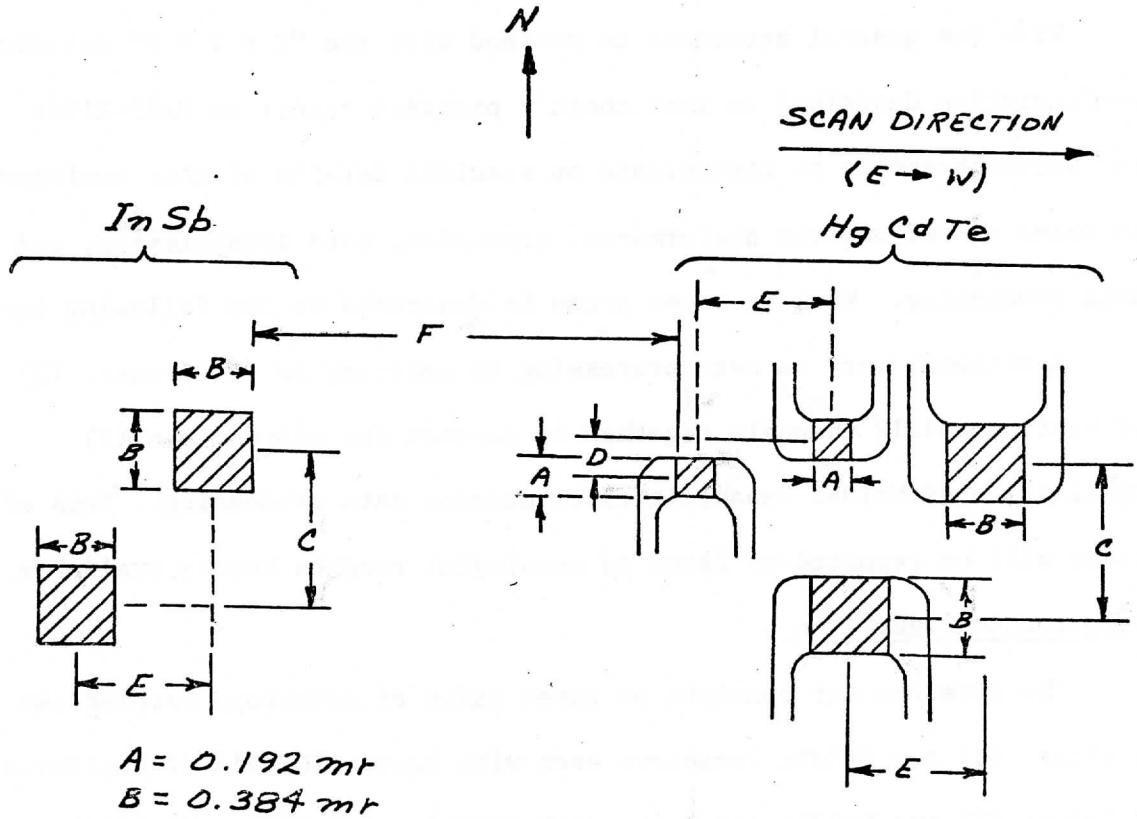


A = 0.192 mr
B = 0.384 mr
C = 0.768 mr
D = 0.192 mr

E = 2(n + 1/2) × 0.04189 mr (SMALLEST n ALLOWED BY LEAD SPACING)

F ≈ 2.1 mr

Figure 1 Detector IGFOV Arrangement

Note that A, D, B/2, and C/4 are equal in angle to the north-south latitude step of the VISSR scan mirror.

to be an odd integral multiple of 0.4189mr (the angle scanned at 100 RPM between samples of alternate detectors of a set).

In order to minimize effects of non-uniform responsivity over the detector surface, electrodes are attached in the E-W direction and bias currents are opposite for members of the same pair. According to SBRC the major responsivity variation is a ramp function aligned with the bias current. By double scanning a given line, once with each detector of a pair, the average responsivity is flat if the bias directions are opposite between the two detectors. The E-W orientation of the bias current was chosen to achieve some smoothing of the ramp response from the presampling filter.

## III. Filter Selection

With the commitment to include InSb detectors band 1 (at the 15μ Q-branch) became vacant. The benefit of including another filter in the 4.3μ band was weighed against the degradation of the 4.3μ window resulting from increasing the cold filter bandpass. After discussions with William L. Smith of NOAA and John Moody of NASA, this filter was dropped and another 15μ band filter was included instead. In addition some readjustments of the low wavenumber $CO_2$ filters and the high wavenumber filters were suggested. The present set of filters recommended for the VISSR Atmospheric Sounder are listed in Table 1.

## IV. Radiometric Performance

### 1. Revised Autocovariance Function

The present plan to leave the S/C presampling filter unchanged at 26 KHz for the upper 3 dB point required new autocovariance functions to use in evaluating noise averaging characteristics as a function of the area averaged. The techniques used are those described in detail in the previous monthly report. A series expansion with 32 ideal bandpass filters

Table 1. VAS Filter Recommendation

| Filter Number | Central Wavenumber ($cm^{-1}$) | Half Bandwidth ($cm^{-1}$) | Transmittance |
|---|---|---|---|
| 1 | 680 | 10 | .60 |
| 2 | 692 | 16 | .60 |
| 3 | 703 | 16 | .60 |
| 4 | 715 | 20 | .60 |
| 5 | 745 | 20 | .60 |
| 6 | 760 | 20 | .60 |
| 7 | 790 | 20 | .60 |
| 8 | 895 | 140 | .65 |
| 9 | 1380 | 40 | .60 |
| 10 | 1490 | 150 | .75 |
| 11 | 2335 | 50 | .60 |
| 12 | 2680 | 440 | .65 |

was used to approximate the power transfer function of the presampling filter and DC restore circuit. The exact transfer function and its series expansion are compared in Figure 2. The resulting autocovariance functions are plotted in Figure 3 for $f_c$ = 10 Hz (InSb) and $f_c$ = 750 Hz (HgCdTe).

These functions were used to calculate relative standard deviations of means for a variety of integrating squares as listed in Table 2.

2. NEN Estimates

A change in IR filters and in the presampling filter specification result in new NEN values as shown in Table 3. The noise equivalent bandwidths ($\Delta f_N$) are calculated from the series summation

$$\Delta f_N = \sum_{k=1}^{32} W_k \, f_{N,k} \text{ , where}$$

$$\Delta f_{N,k} = fmax_k - fmin_k + f_c \ln \frac{fmax_k}{fmin_k}$$

and where $fmax_k$, $fmin_k$ and $W_k$ are the kth parameters in the 32 term series expansion of the noise power transfer function of the presampling filter and DC restore circuit. Transmission values are based on option 5 optics (in-line refractive, with field lens), as described in SBRC's Monthly Progress Report No. 1 on NAS5-21139.

3. Spin Requirements for Dwell Sounding

Spin requirements for the operational mode of dwell sounding are tabulated in Table 4. The objective of this mode is to return useful soundings at 150 km intervals. The corresponding radiometric requirement is that NEN values needed for inversion be obtained at a resolution of approximately 30 km for bands 2-10 and 12 and at a resolution of about 150 km for bands 1 and 11. This would normally insure accurate clear column radiances every 150 km.

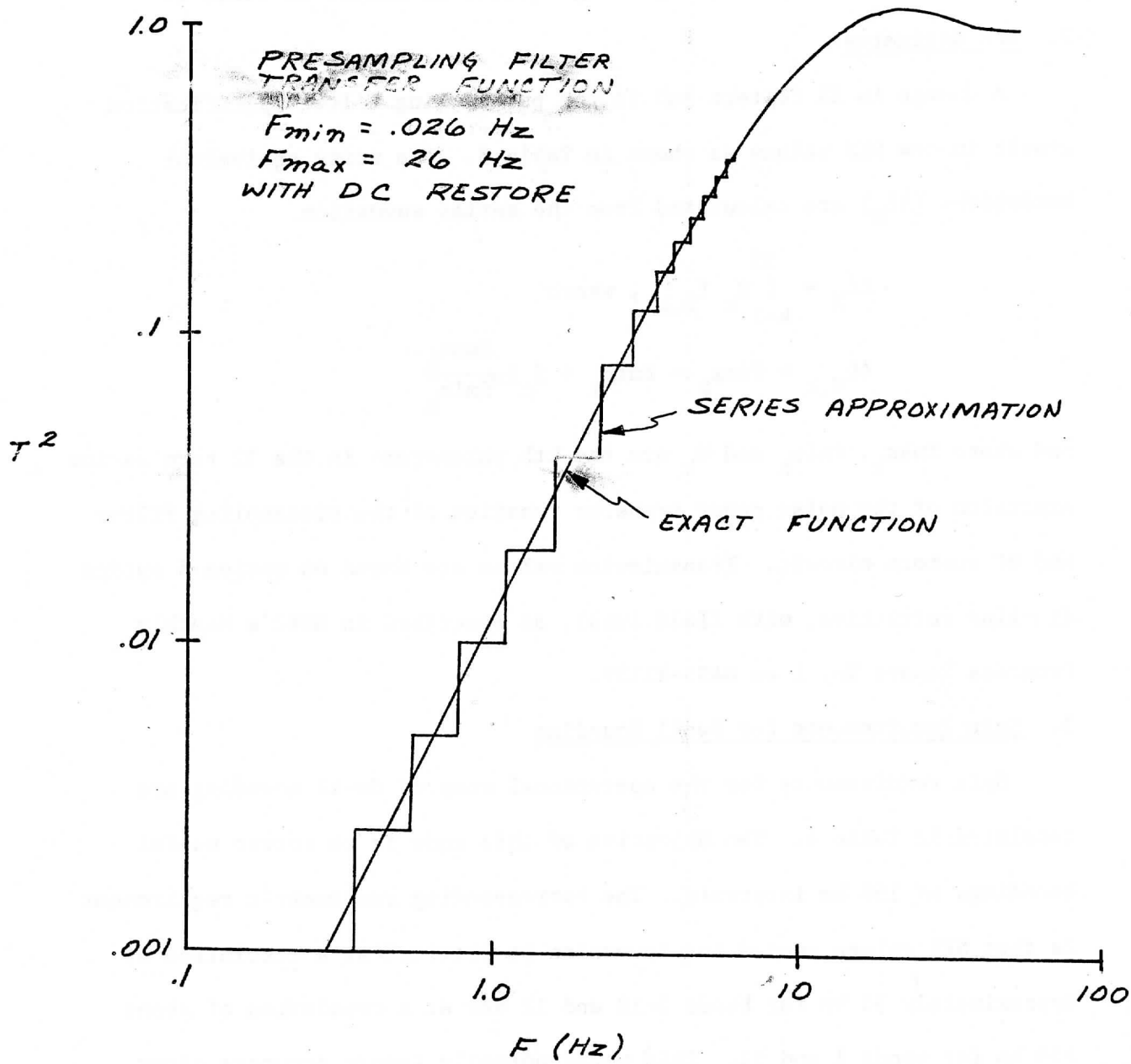
PRESAMPLING FILTER
TRANSFER FUNCTION
Fmin = .026 Hz
Fmax = 26 Hz
WITH DC RESTORE
SERIES APPROXIMATION
EXACT FUNCTION
T²
1.0
.1
.01
.001
.1
1.0
10
100
F (Hz)

Figure 2

Figure 3 - With D.C. Restore, with Bump
Fmin = 0.026 Hz, Fmax = 26 KHz

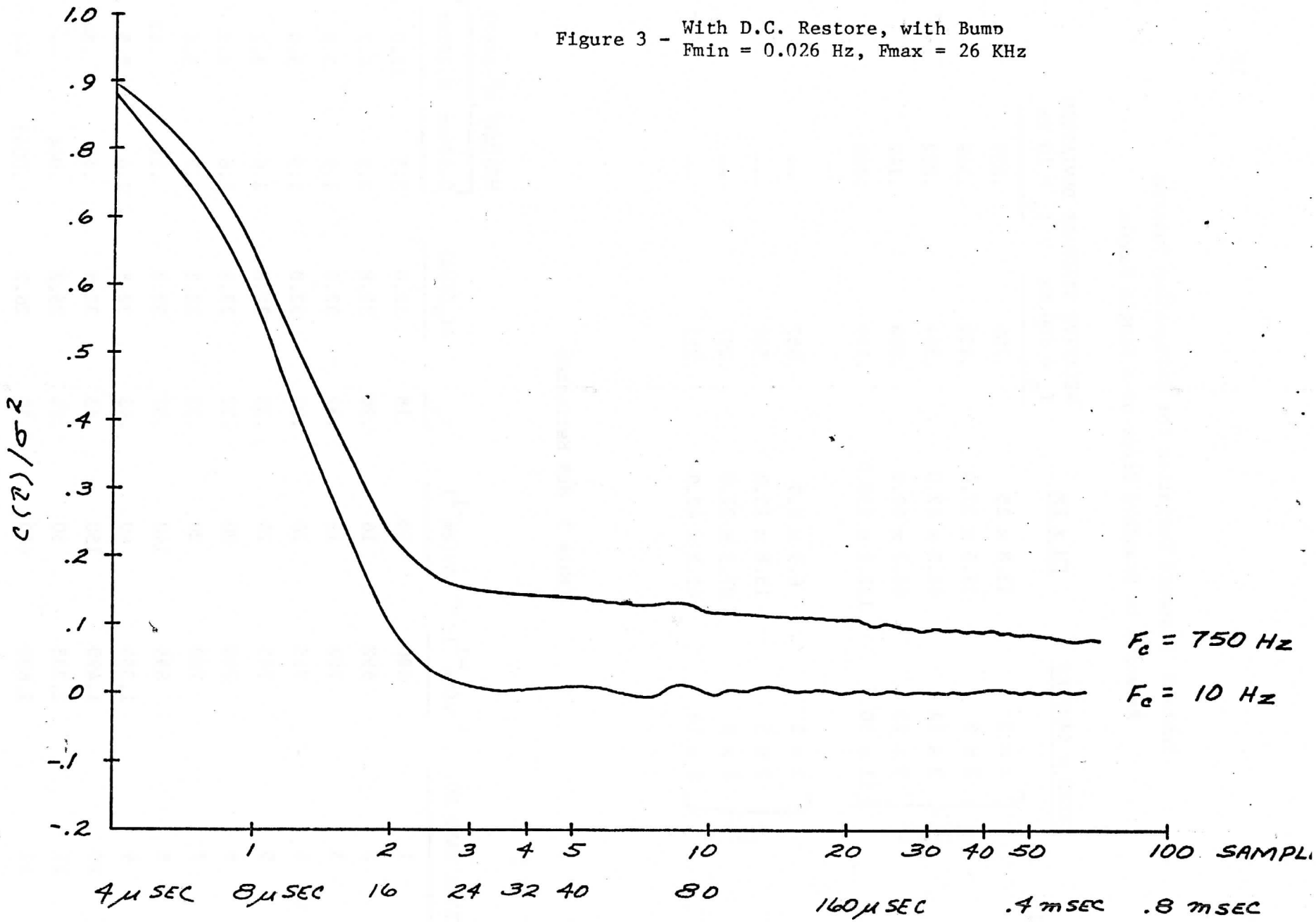

Table 2 Standard Deviation for Integrating Squares Relative to Standard Error of a Single Sample

| | LINES x SAMPLES | KM x KM | RELATIVE STANDARD DEVIATION $f_c$ = 750 Hz | $f_c$ = 10 Hz |
|---|---|---|---|---|
| 0.384mr | 1 x 5 | 13.8 x 15 | .706 | .639 |
| | 2 x 9 | 27.5 x 27.0 | .420 | .349 |
| | 3 x 14 | 41.2 x 42.0 | .304 | .232 |
| | 5 x 23 | 68.7 x 69.0 | .208 | .142 |
| | 11 x 50 | 151.2 x 150.0 | .119 | .066 |
| 0.192mr | 1 x 2 | 6.9 x 6.0 | .907 | -- |
| | 2 x 5 | 13.8 x 15.0 | .500 | -- |
| | 4 x 9 | 27.5 x 27.0 | .297 | -- |
| | 6 x 14 | 41.2 x 42.0 | .215 | -- |

Table 3 NEN Estimates

| FILTER BAND NO. | $\nu(cm^{-1})$ | $\Delta\nu(cm^{-1})$ | $\tau_\nu$ | $\Delta f_N$(KHz) | NEN(mW/ $m^2$-ster) 0.384mr | 0.192mr |
|---|---|---|---|---|---|---|
| 1 | 680 | 10 | .18 | 32.8 | 5.5 | 11.0 |
| 2 | 692 | 16 | .26 | 32.8 | 2.3 | 4.7 |
| 3 | 703 | 16 | .32 | 32.8 | 1.9 | 3.8 |
| 4 | 715 | 20 | .32 | 32.8 | 1.5 | 3.0 |
| 5 | 745 | 20 | .32 | 32.8 | 1.6 | 3.2 |
| 6 | 760 | 20 | .32 | 32.8 | 1.6 | 3.3 |
| 7 | 790 | 20 | .32 | 32.8 | 1.7 | 3.4 |
| 8 | 895 | 140 | .37 | 32.8 | .21 | .43 |
| 9 | 1,380 | 40 | .43 | 32.8 | 1.4 | 2.8 |
| 10 | 1,490 | 150 | .43 | 32.8 | .42 | .84 |
| 11 | 2,335 | 50 | .24 | 26.2 | .044 | -- |
| 12 | 2,680 | 440 | .30 | 26.2 | .0045 | -- |

Table 4 Dwell Sounding Spin Requirements

| BAND | NEN/SAMPLE ($mW/m^2$-ster) | NEN OBTAINED ($mW/m^2$-ster) @ REQUIRED RESOLUTION | REQUIRED NEN ($mW/m^2$-ster) | REQUIRED SPINS/BAND |
|---|---|---|---|---|
| 1 | 5.5 | 0.65 @ 150 km | 0.25 | 7 |
| 2 | 2.3 | 0.97 @ 27 km | 0.25 | 15 |
| 3 | 1.9 | 0.80 @ 27 km | 0.25 | 10 |
| 4 | 1.5 | 0.63 @ 27 km | 0.25 | 7 |
| 5 | 1.6 | 0.67 @ 27 km | 0.25 | 7 |
| 6 | 1.6 | 0.67 @ 27 km | 0.25 | 7 |
| 7 | 1.7 | 0.71 @ 27 km | 0.25 | 8 |
| 8 | .21 | 0.09 @ 27 km | 0.25 | 1 |
| 9 | 1.4 | 0.59 @ 27 km | 0.15 | 6 |
| 10 | .42 | 0.18 @ 27 km | 0.10 | 3 |
| 11 | .044 | .0029 @ 150 km | 0.002 | 2 |
| 12 | .0045 | 0.0015 @ 27 km | 0.002 | 1 |
| | | | TOTAL SPINS FOR SOUNDING/DWELL | 74 |

In Table 4 the second column (NEN/SAMPLE) is obtained from Table 3; the third column is derived from the first and the results of Table 2, assuming complete nonoverlapping coverage with 0.384mr detectors; and the fourth column (SPINS/BAND) is the number of scans per band of the same geographical area that must be averaged in order to reduce noise to a tolerable level.

## V. Scanning Modes

The VISSR sounder will have programmable scanning and filter stepping capabilities. Two distinct formats are now planned for implementation: imaging (also called imaging/sounding); and dwell sounding. In the first mode the VISSR latitude step occurs once per spin; in the second the scan mirror dwells on a single line for a programmed number of spins. The basic operation of each is explained in the following subsections.

### 1. Imaging/Sounding Operation

The basic repeated program sequence for this mode consists of 8 spins. Since the small HgCdTe detectors scan two 0.192mr swaths/spin they must be used for four of the eight spins (during every other spin) to obtain a complete image in the 11.2μ band. During the remaining four spins out of each eight other filters and other detectors can be selected. Since the large detectors scan two 0.384mr swaths each spin, it is possible to obtain complete spatial coverage at this resolution in one other spectral channel by using only two of the remaining four spins in the sequence. A complete 0.384mr image can also be obtained in a third spectral interval using the last two spins.

The scan pattern for imaging in three spectral bands (11.2μ @ 0.192mr, 3.7μ @ 0.384mr, and 6.7μ @ 0.384mr) is displayed in Figure 4. The N-S motion of the detector array is indicated by vertical displacements, and

# SCAN PATTERN FOR IMAGE - SOUND MODE

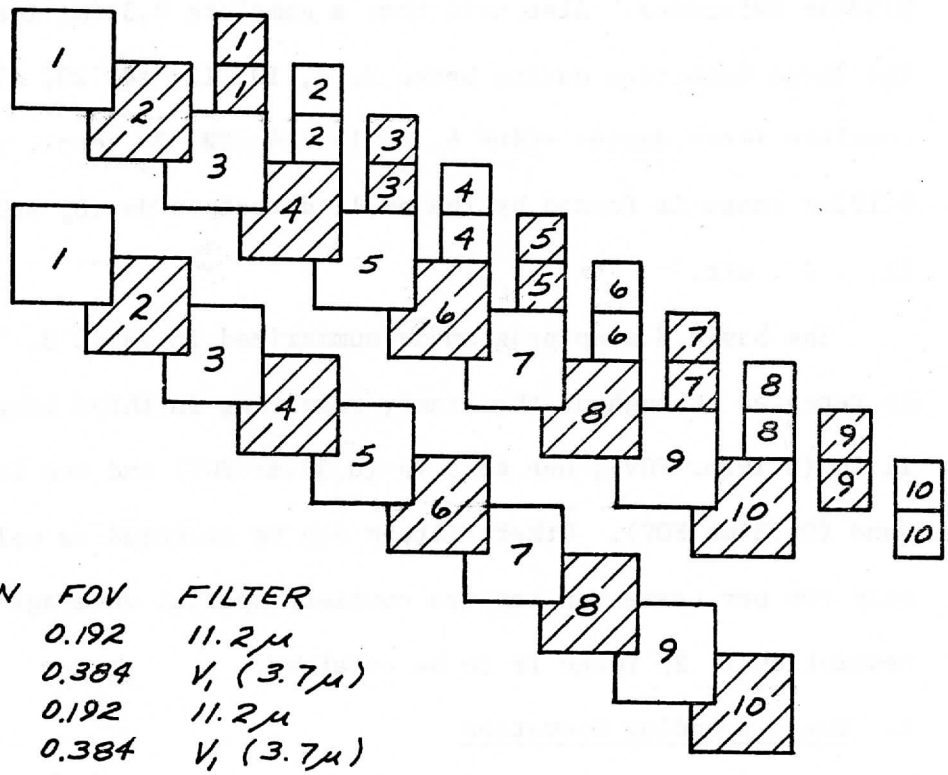


| SPIN | FOV | FILTER |
|---|---|---|
| 1 | 0.192 | 11.2 $\mu$ |
| 2 | 0.384 | $V_1$ (3.7 $\mu$) |
| 3 | 0.192 | 11.2 $\mu$ |
| 4 | 0.384 | $V_1$ (3.7 $\mu$) |
| 5 | 0.192 | 11.2 $\mu$ |
| 6 | 0.384 | $V_2$ (6.7 $\mu$) |
| 7 | 0.192 | 11.2 $\mu$ |
| 8 | 0.384 | $V_2$ (6.7 $\mu$) |

shading is used to indicate which detectors are "on", i.e. whether large or small detectors are being sampled. The number in each detector box indicates the relative spin number in the sequence. Note that for simplicity only one pair of boxes is used to represent both InSb and HgCdTe 0.384mr detectors. Also note that a complete 0.384mr image is formed by the large detectors during spins 2, 4, 10, 12, 18, 20, etc., and another complete image during spins 6, 8, 14, 16, 22, 24, etc., while a complete 0.192mr image is formed by the small detectors during spins 1, 3, 5, 7, 9, 11, . . . etc.

The basic 8 step program is summarized in Table 5. This program is repeated throughout the frame, resulting in three images: one at 11.2μ (0.192mr FOV); one at 3.7μ (0.384mr FOV) and one in the 6.7μ $H_2O$ band (0.384mr FOV). Other filters can be selected as well, but at most only two per frame can achieve complete spatial coverage if the high resolution 11.2μ image is to be retained.

2. Dwell Sounding Operation

The dwell sounding program includes two distinct submodes: (1) latitude stepping at 1 step per spin while imaging with the 0.192mr HgCdTe detectors in the 11.2μ band; and (2) sequencing through all 12 filters with a programmed number of spins per spectral band while the VISSR scan mirrors dwells at the current latitude position. The complete repeated program consists of three submodes specified as follows: steps prior to dwell - dwell spin program - steps following dwell. The only advantage of two stepping specifications of this type is an improved scanning efficiency for very short frame heights. The dwell program parameters are (1) detector set to be used and (2) spins per dwell for each of the twelve filters (except for bands 11 and 12 which must always use the InSb detectors).

Table 5 Three Band Image Program

| Spin No. | Filter | Detector Pair | FOV |
|---|---|---|---|
| 1 | 8 (11.2μ) | small HgCdTe | 0.192mr |
| 2 | 12 (3.7μ) | InSb | 0.384mr |
| 3 | 8 (11.2μ) | small HgCdTe | 0.192mr |
| 4 | 12 (3.7μ) | InSb | 0.384mr |
| 5 | 8 (11.2μ) | small HgCdTe | 0.192mr |
| 6 | 10 (6.7μ) | large HgCdTe | 0.384mr |
| 7 | 8 (11.2μ) | small HgCdTe | 0.192mr |
| 8 | 10 (6.7μ) | large HgCdTe | 0.384mr |

By combining stepping and dwell submodes it is possible to achieve scan patterns which produce 50% spatial coverage each pass (Figure 5), or complete spatial coverage with double scanning (Figure 6). In the latter case, to achieve complete spatial coverage, the present programming capabilities require using both upper and lower large detectors to scan the same geographical area. Note, for example, that in Figure 6 the swath scanned by the lower 0.384mr detector during spins 3-40 is also scanned by the upper 0.384mr detector during spins 53-90. Also note that in all cases each 0.192mr swath is scanned by both upper and lower 0.192mr detectors (11.2μ filter in place) during stepping between dwells.

Note that in Figures 5 and 6 "on" detectors are shaded and numbered to indicate relative spin numbers while "on". As in Figure 4 the latitude stepping is indicated by the vertical position of the FOV pattern, and only one set of large detectors is diagrammed for simplicity.

A more efficient program for complete spatial coverage (without double scanning) is depicted in Figure 7. At present this program capability has not been implemented to avoid complicating the VAS processor.

## VI. Data Transmission

Since the present VAS detector configuration requires sampling only two detectors per line and since the present S/C to CDA link already handles two IR detector channels (primary and redundant), no problem is anticipated in getting all raw VAS data to the CDA station.

However, the stretched link (CDA to S/C to SFSS) is presently configured to carry only one IR channel (either primary or redundant detector outputs or the average). Thus some modification of the stretched link is required to transmit both channels of raw VAS data to the SFSS in real time. This could be done simply by doubling the IR bit rate, since

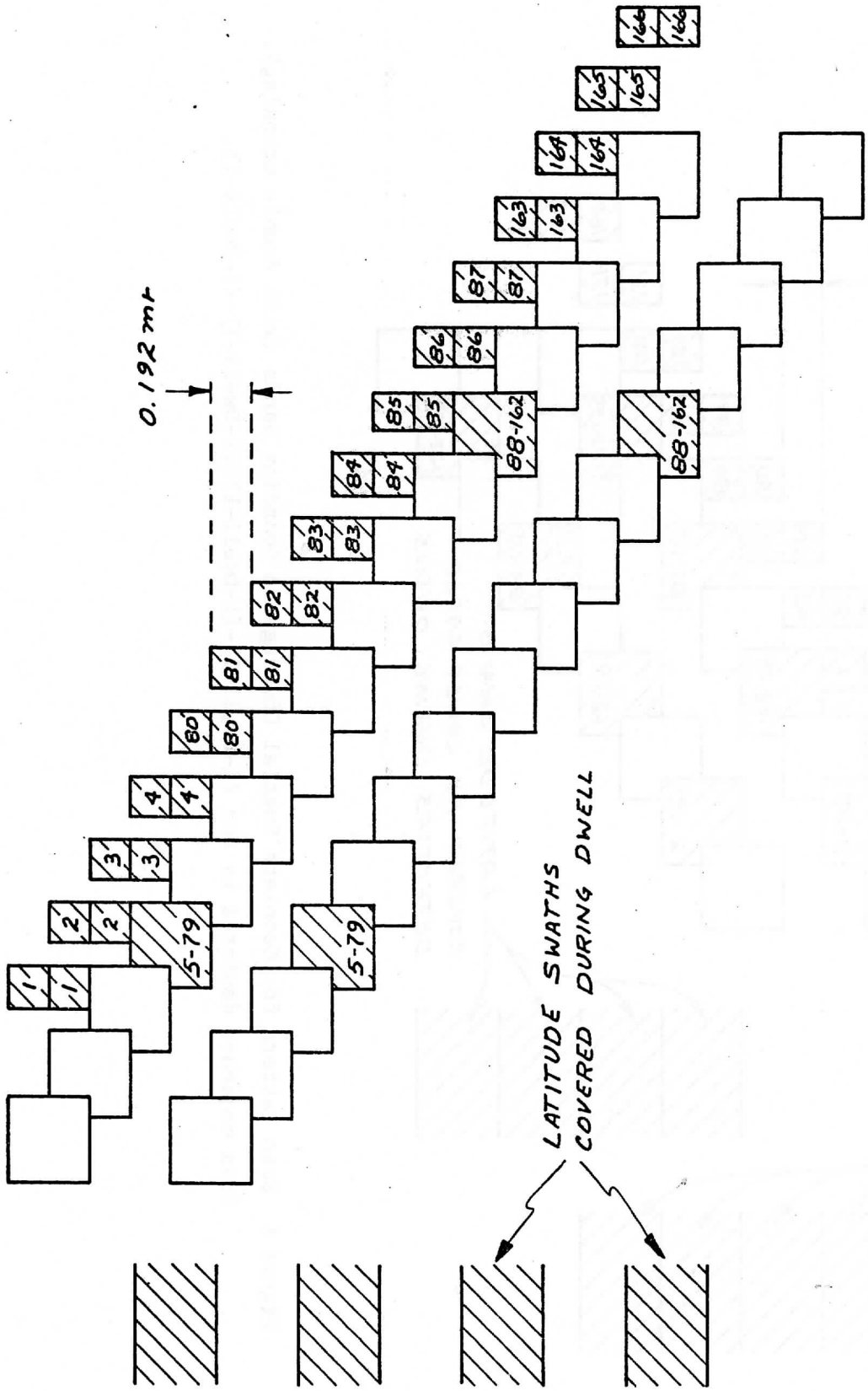


Figure 5 Scan Pattern for 50% Spatial Coverage in Sounding Bands.
Scan sequence depicted is for (4-Dwell-4)-(4-Dwell-4).

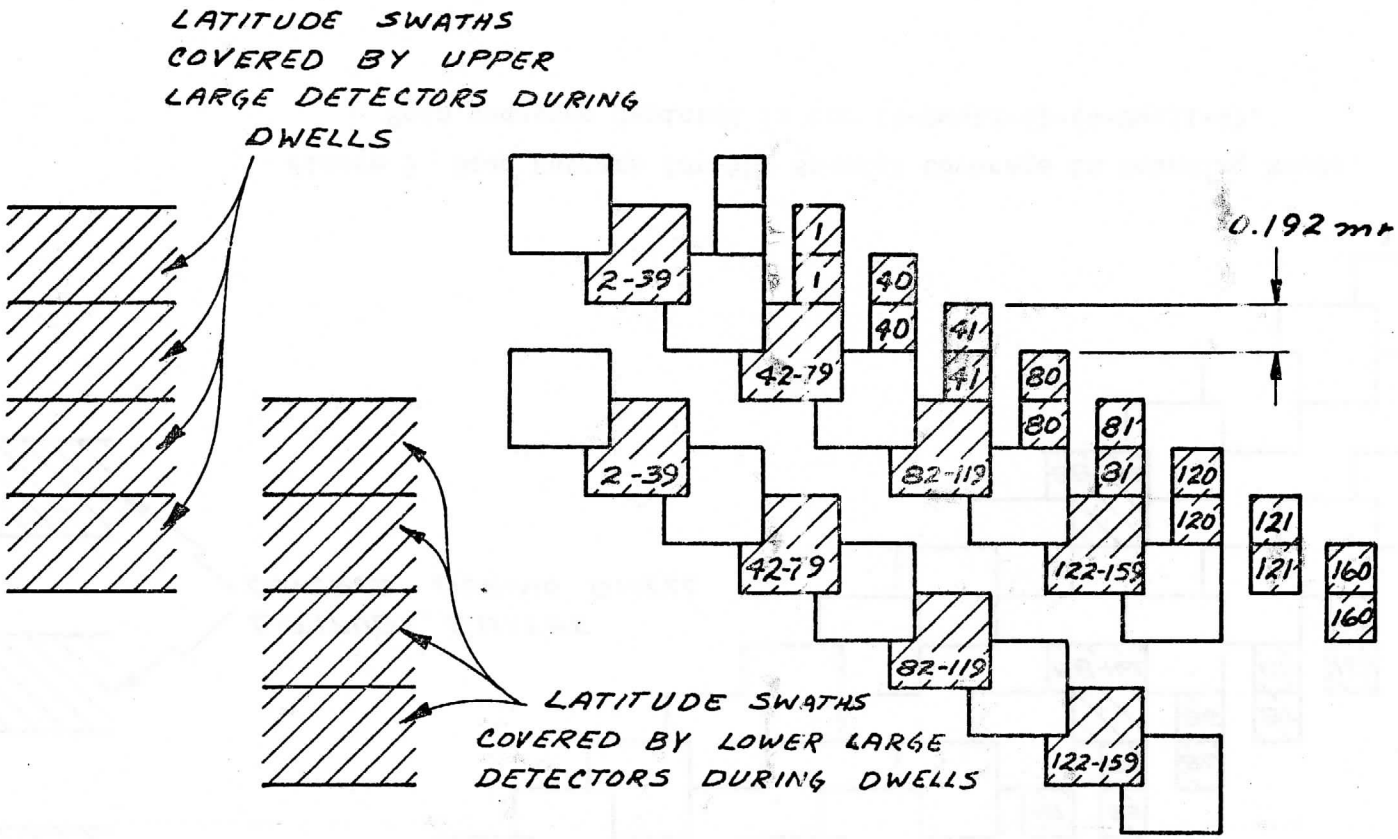


Figure 6 Scan Pattern for Complete Spatial Coverage in Sounding Bands (with double scanning). Scan sequence depicted is for (1-Dwell-1)-(1-Dwell-1)-(1-Dwell-1)-(1-Dwell-1).

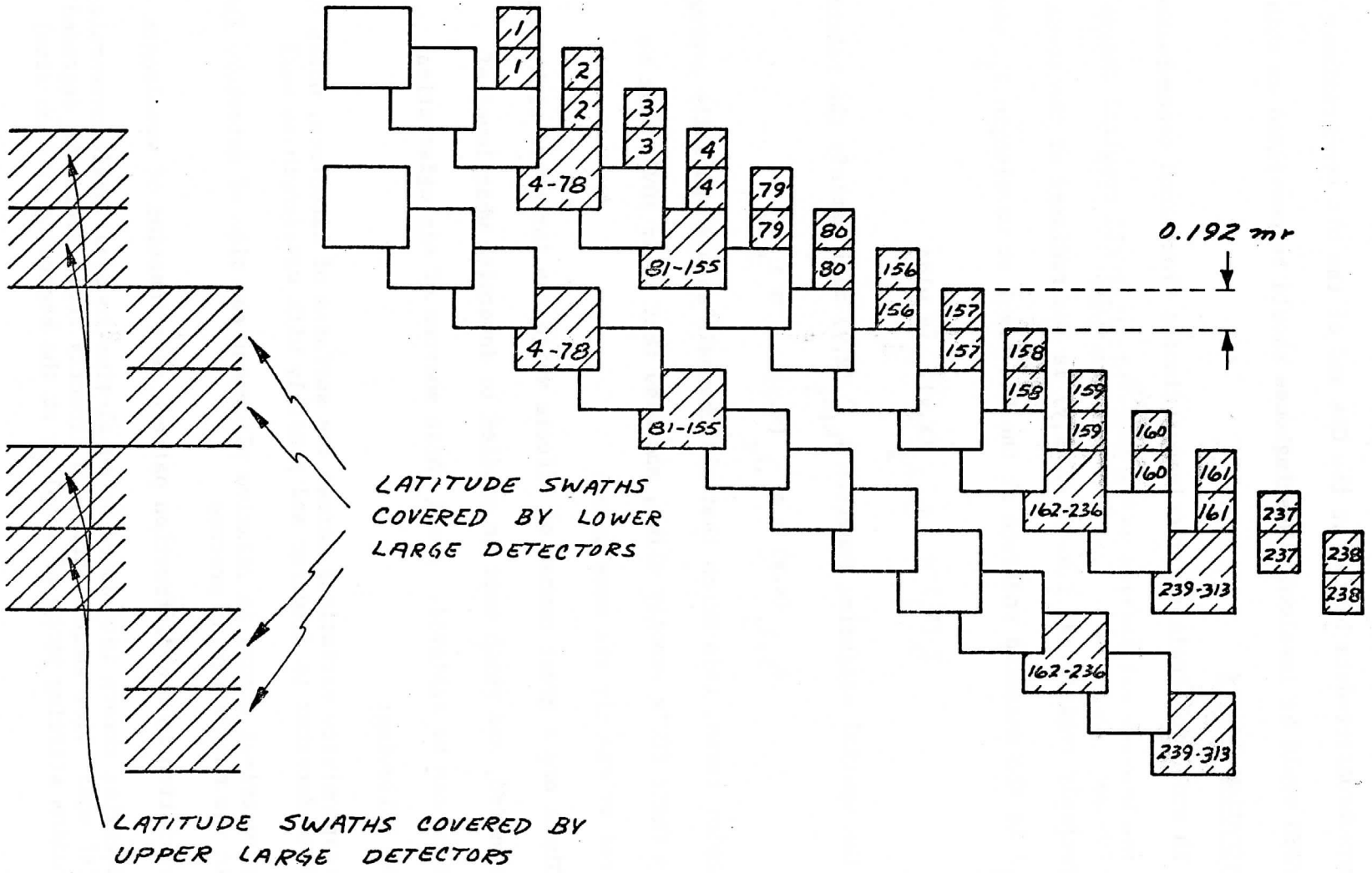


Figure 7 Most efficient scan pattern for complete spatial coverage (above) uses the repeated program 4-Dwell-2-Dwell, which is not within present capabilities. The depicted sequence is (4-Dwell-2-Dwell)-(4-Dwell-2-Dwell). Note that there is no double scanning of the same geographical area by upper and lower

it would still be well below the bit rate for 1/2 n.mi. visible data. It appears that relatively minor modifications of formatting programs in the synchronizer-data buffer at the CDA and of the bit synchronizers at the SFSS would be involved. Westinghouse should be consulted on this point.

## VII. Registration Errors

In order to obtain clear column radiances from cloud contaminated radiances with the highest reliability it is desirable that all spectral channels be precisely registered, i.e. if $I_\lambda(x,y)$ is the radiance of the scene and $I_k(\lambda_j)$ is the measured radiance at the kth pixel at wavelength $\lambda_j$, where

$$I_k(\lambda_j) = \phi_{k,\lambda_j}(x,y) I_{\lambda_j}(x,y)\,dA$$

then the spatial weighting function $\phi_{k,\lambda_j}(x,y)$ must satisfy the relation

$$\phi_{k,\lambda_j}(x,y) = \phi_{k,\lambda_i}(x,y) \qquad \forall\ \lambda_j,\lambda_i$$

In simpler terms, this means that all channels should spatially average within their FOV's exactly alike, and also that their FOV's must be centered at exactly the same point.

There are a great number of effects which can interfere with perfect registration, and which must be studied to determine what level of precision can be achieved. Among these sources of misregistration are the following:

(1) responsivity variations across the surfaces of detectors, which varies, from detector to detector and possibly with wavelength as well

(2) geometrical errors in relative placement and size of detectors introduced in the manufacturing process

(3) variation in the diffraction pattern as a function of wavelength

(4) location errors introduced by equal-time to equal angle conversion (if equal time samples are used directly registration is degraded by random starting phase of sampling at the beginning of each line)

(5) location errors introduced by deviations of the latitude step increment from 0.192mr.

(6) motion of clouds and/or apparent motion of the earth in the time interval used to sequence through all channels.

Information obtained from SBRC regarding item (2) is summarized in Table 6. Characteristic HgCdTe reponsivity variations, according to SBRC also, are shown in Figure 8. The specification of reverse bias, discussed in Section II, results in averaging of up and down ramps. According to SBRC the residual variation of responsivity in the x direction (Figure 8) is probably of the same order of magnitude as the variation in the y direction, i.e. about 25% P-P. A computer simulation of this size variation was made to determine its effect on radiance averages over a 30 km integrating square. (The details are quite similar to those described in the October progress report.) The results, shown in Figure 9, indicate an RMS error of about 0.6% of the difference between the clear radiance and cloud radiance when the scene is approximately 50% clear. For a 50 erg/etc difference this amounts to a radiance error of 0.3 erg/etc. More realistic tests including difraction and presample filtering which smooth the responsivity variations would reveal somewhat smaller errors due to responsivity variations.

Further tests will be made and reported on in the future. We are now beginning a test of a data processing algorithm to reduce errors due to relative N-S misalignment of detectors. Results should be available in time for the December report.

Table 6 Geometrical Errors in Detector Array Fabrication

| ITEM | EQUIVALENT ANGULAR ERROR |
|---|---|
| Centroid Position Error on a Substrate | ± 3μr (InSb)<br>± 7μr (HgCdTe) |
| North-South Alignment of InSb Array Relative to HgCdTe Array | ± 30μr (without correction)<br>± 15μr (with cooler rotation) |
| Detector Size Error | ± 14μr (in linear dimensions) |

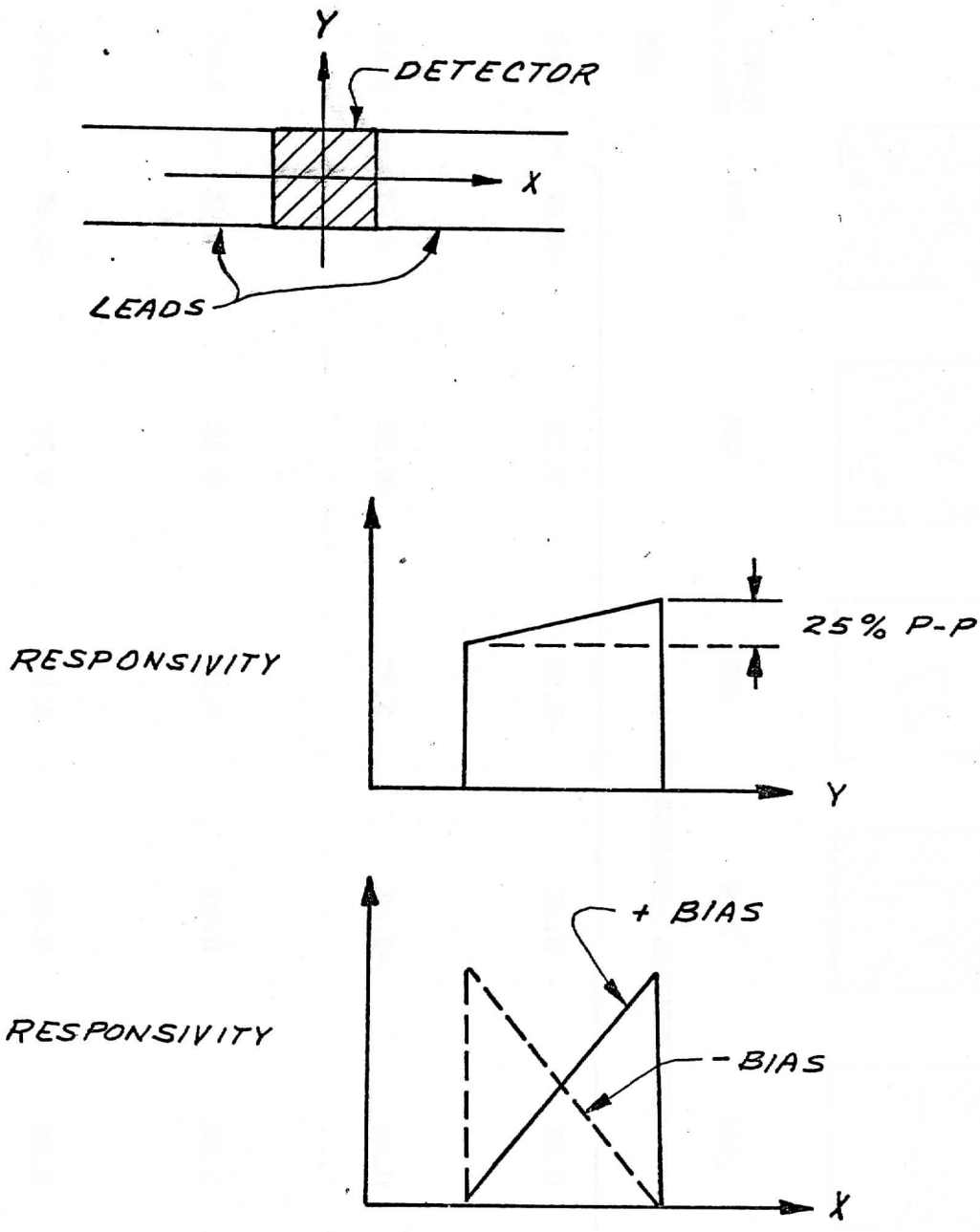


Figure 8 HgCdTe Detector Responsivity Variations

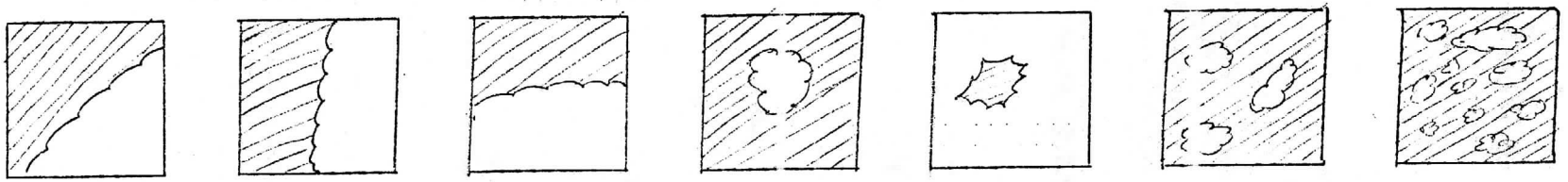

ENE

IGHTS

| | | | | | | | |
|---|---|---|---|---|---|---|---|
| 1 1 / 1 1 | .340 | .500 | .500 | .389 | .625 | .451 | .597 |

CLOUD FRACTION

DIFFERENTIAL RADIANCE ERRORS

RMS

| | | | | | | | | |
|---|---|---|---|---|---|---|---|---|
| 3 3 / 4 4 | 0.7% | 0.0% | 0.0% | 0.8% | -0.6% | 0.7% | -0.6% → | 0.6% |
| 4 4 / 3 3 | -1.4% | 0.0% | 0.0% | -0.8% | 0.6% | -0.7% | 0.6% → | 0.6% |
| 3 4 / 3 4 | 0.7% | 0.8% | 0.0% | 0.0% | 0.0% | -0.1% | 0.2% → | 0.4% |
| 4 3 / 4 3 | -1.4% | -0.8% | 0.0% | 0.0% | 0.0% | 0.1% | -0.2% → | 0.6% |
| | ↓ | ↓ | ↓ | ↓ | ↓ | ↓ | ↓ | ↓ |
| RMS | 1.1% | 0.6% | 0.0% | 0.6% | 0.4% | 0.5% | 0.4% → | 0.6% |

Figure 9 Simulation Results for 25% P-P Responsivity Variations

ERRORS ARE EXPRESSED IN TERMS % OF THE DIFFERENCE $I_{CLD.} - I_{CLEAR}$.